Gold Nanoparticles Promote Osteogenic Differentiation of Mesenchymal Stem Cells through p38 MAPK Pathway

Changqing Yi,[†,‡,⊥] Dandan Liu,[†,§,⊥] Chi-Chun Fong,[‡] Jinchao Zhang,[§,*] and Mengsu Yang[†,‡,*]

[†]Key Laboratory of Biochip Technology, Biotech and Health Centre, Shenzhen Research Institute of City University of Hong Kong, Shenzhen, China, [‡]Department of Biology and Chemistry, City University of Hong Kong, Hong Kong, China, and [§]College of Chemistry and Environmental Science, Hebei University, Baoding, China. [⊥]C. Q. Yi and D. D. Liu contributed equally to this work.

ABSTRACT Understanding the interaction mechanisms between nanomaterials and biological cells is important for the control and manipulation of these interactions for biomedical applications. In this study, we investigated the cellular effects of gold nanoparticles (AuNPs) on the differentiation of mesenchymal stem cells (MSCs) and the associated molecular mechanisms. The results showed that AuNPs promoted the differentiation of MSCs toward osteoblast cells over adipocyte cells by inducing an enhanced osteogenic transcriptional profile and an attenuated adipogenic transcriptional profile. AuNPs exerted the effects by interacting with the cell membrane and binding with proteins in the cytoplasm, causing mechanical stress on the MSCs to activate p38 mitogen-activated protein kinase pathway (MAPK) signaling pathway, which regulates the expression of relevant genes to induce osteogenic differentiation and inhibit adipogenic differentiation.

KEYWORDS: gold nanoparticles · mesenchymal stem cells · osteogenic differentiation · adipogenic differentiation · mitogen-activated protein kinase pathway

One of the strategies for improving bone tissue engineering is to stimulate the osteogenic differentiation and bone forming properties of osteo-progenitor cells. Mesenchymal stem cells (MSCs) have been considered the progenitor cells for the skeletal tissues, and they can differentiate along multiple lineages such as osteoblasts, chondrocytes, and adipocytes.[1−6] Because of their ability to be cultured for successive passages and multilineage differentiation, MSCs have attracted particular attention in the field of regenerative medicine. Recently, there is accumulating evidence that nanoscale materials can facilitate stem cell therapy and bone tissue engineering.[7−15] Synthetic polymer materials have been fabricated into nanoscale structures in order to stimulate the matrix environment in which seeded cells could be accommodated to proliferate and differentiate toward desired lineages.[7−10] Well-ordered $SrTiO_3$ nanotube arrays capable of releasing strontium (Sr) have been demonstrated to enhance osteogenesis.[11] MSCs cultured on glass substrates coated with bionanoparticles, such as turnip yellow mosaic virus (TYMV) and tobacco mosaic virus (TMV), showed an early maturation and mineralization when differentiating into osteoblasts-like cells.[12,13] Further modification of TMV with phosphate resulted in a significantly higher up-regulation of osteo-specific genes as compared to unmodified TMV particles.[14] Aqueous suspensions of nanoparticles have also been demonstrated to promote the differentiation of MSCs toward osteoblasts.[15−17] Davis and co-workers showed that it was sufficient to stimulate MSC differentiation and bone matrix production in the absence of osteogenic media by modifying human MSCs directly in aqueous suspension with amino acid-functionalized calcium phosphate nanoparticles.[17] Although the potential use of nanomaterials in modulating MSC differentiation is evident, the interactions between nanoparticles and MSCs have not been studied in detail, and the molecular mechanisms governing MSC self-renewal and differentiation in the presence of nanoparticles remain largely unknown.

In this study, we investigated the effects of gold nanoparticles (AuNPs) on the differentiation of MSC and the associated molecular mechanisms. The cellular effects of AuNPs on the proliferation, osteogenic differentiation, adipogenic differentiation, and mineralization of MSCs were evaluated by MTT assay, alkaline phosphatase (ALP) activity assay, Oil red O staining assay, and Alizarin red S staining assay, respectively. In addition, scanning electron microscopy (SEM) and transmission electron microscopy (TEM) were used to characterize the morphology and ultrastructural change of MSCs during osteogenic differentiation in the presence of AuNPs, respectively.

*Address correspondence to bhmyang@cityu.edu.hk, jczhang6970@yahoo.com.cn.

Received for review June 18, 2010 and accepted October 18, 2010.

Published online October 28, 2010.
10.1021/nn101373r

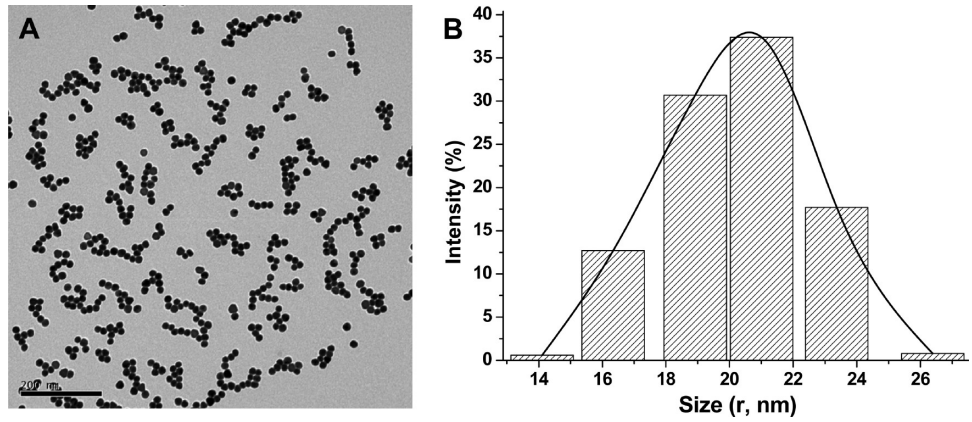

Figure 1. TEM image (A) and size distribution histogram (B) of AuNPs.

Cellular assay results demonstrated that AuNPs promoted the differentiation of MSCs toward osteoblasts over adipocytes with increasing ALP activity and mineralization of the extra-cellular matrix. On the basis of the observed cellular effects and previous reports,[18−20] we hypothesized that AuNPs may interact with the cells by membrane adsorption and subsequent internalization through endocytosis, possibly serving as mechanical stimuli on MSCs to activate mechanosensitive signaling pathway in the cells and thus induce osteogenic differentiation. Real-time reverse transcriptase polymerase chain reaction (RT-PCR) and Western blotting assays were designed to verify the hypothesis at the molecular level by determining the expression of genes and proteins related to pathways stimulated by mechanical stress and the expression of osteogenic and adipogenic biomarkers of MSCs upon interaction with AuNPs. The results showed that the interaction of MSCs with AuNPs may lead to the activation of the p38 mitogen-activated protein kinase pathway (MAPK) signaling pathway and the up-regulation of osteogenic genes and the down-regulation of adipogenesis specific genes.

RESULTS AND DISCUSSIONS

An aqueous dispersion of AuNPs was prepared by citrate reduction.[21] According to the model by Chow and Zukoski,[22] an increase in the concentration of citrate ions would decrease the final size of colloidally stable particles and increase the zeta potential of particles. As shown in the TEM images (Figure 1A), the as-prepared AuNPs are rather monodisperse and spherical in shape, with an estimated average diameter of 20 nm. Dynamic light scattering (DLS) measurements confirmed that the average diameter of AuNPs is 20 ± 2 nm (Figure 1B), and the zeta potential is −58.76 mV. Energy-dispersive X-ray (EDX) spectra confirmed that the only composition of nanoparticles was gold (Supporting Information, Figure S1).

Differentiation of pluripotent progenitor MSCs into osteoblasts is a crucial step of osteogenesis. The appearance of ALP activity is an early phenotypic marker for osteogenic differentiation of MSCs, and mineralized nodule formation is a phenotypic marker for the last stage of mature osteoblasts.[23] Generally, ALP activities were expressed after *in vitro* osteogenic induction for 7 days, while later positive ALP staining was seen after 14 days of osteogenic induction.[24] The effects of AuNPs on osteogenic differentiation of MSCs cultured for 7, 10, and 14 days in the presence of osteogenetic supplement (OS) were assessed by measuring their ALP activity normalized to total protein content. The results showed that the higher the concentration of AuNPs was, the stronger was the promotion of osteogenic differentiation of MSCs. On day 14, ALP activity of MSCs treated by all concentrations of AuNPs was dramatically increased compared with that of day 7 and day 10 (Figure 2A). These results indicated a substantial increase of ALP activity in MSCs upon treatment of AuNPs in dose- and time- dependent manners.

Since osteoblast nodes formed and reached a peak when osteoblasts mineralized after 2−3 weeks culture,[25] the mineralized function of the MSCs upon treatment with AuNPs and OS for 9, 15, and 21 days were investigated using Alizarin red S (ARS) staining assay (Figure S2A-2C). NaF at 1.0 μM was used as positive control, which promoted mineralization of MSCs by 12%, 35%, and 42% on day 9, day 15, and day 21, respectively. AuNPs showed a similar promotive effect on the mineralization of MSCs. The formation of mineralized nodules in MSCs upon AuNPs treatment was evaluated by coupling the number count of node formation with quantitation of ARS deposition, which increased in dose- and time-dependent manners. A greater than 45% increase in the formation of mineralized nodules in MSCs upon AuNPs treatment at the dosage of 1.0 nM AuNPs was observed on day 21 (Figure 2B).

The morphological change of MSCs during osteogenic differentiation was investigated using SEM. MSCs adhered to substrates by means of thin cytoplasmic digitations or filopodia, and the cells flattened and expanded cytoplasmic extensions over the entire surface.[10,12] When cultured in basal medium without the addition of OS and AuNPs, the cells displayed a spin-

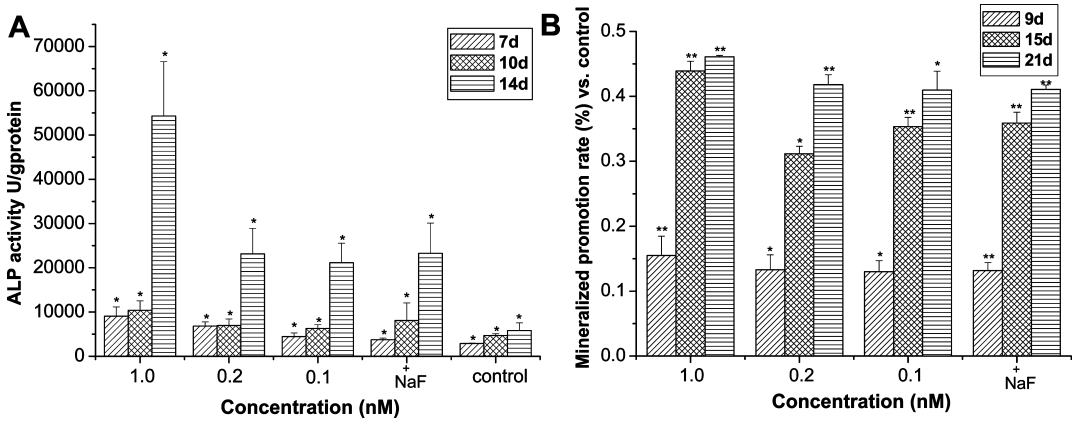

Figure 2. (A) Effects of AuNPs on the ALP activity of MSCs. Results are mean ± SD of the triplicate experiments: (*) $p < 0.01$. NaF at 1.0 μM was used as a positive control. (B) Effects of AuNPs on the mineralized nodule formation of MSCs. Mineralization quantitated by elution of alizarin red S from stained mineral deposits. Results are mean ±SD of the triplicate experiments, (*) $p < 0.05$, (**) $p < 0.01$; 1.0 μM NaF was used as positive control.

dly, fibroblast-like morphology and formed clusters, which is the normal phenotype behavior of MSCs (Figure 3A−C). As the cells differentiated into osteoblasts in the presence of OS with and without the treatment of AuNPs, they started depositing matrix on the surface. SEM images showed that the whole surface was covered with a network of well-spread cells which acquired a more polygonal morphology (Figure 3D,G). The cellular aggregation resulted in the formation of nodular structures (Figure 3E,H). High magnification SEM images showed the long pseudopodia and multilayered cells with various sizes and shapes (Figure 3F,I). The cells formed a dense network, suggesting that AuNPs promoted osteoblast functionality with increasing ALP activity and matrix production.[26] Both the SEM and the cellular assay results demonstrated a substantial promotion of osteogenic differentiation of MSCs upon their interactions with AuNPs.

Because of the reciprocal relationship between osteogenic and adipogenic differentiation of MSCs, it is possible that the promotion of MSC osteogenic differentiation by AuNPs occurs concurrently with the inhibi-

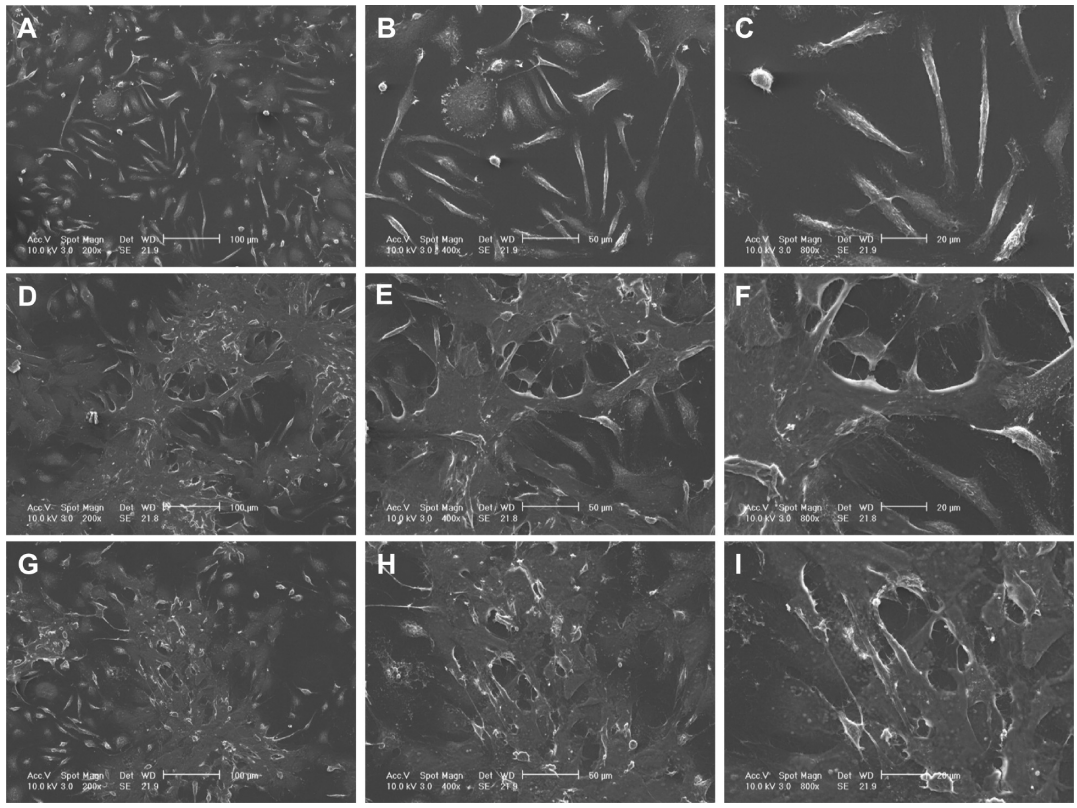

Figure 3. SEM images of MSCs after 7 days culture. (A−C) MSCs were cultured in the absence of AuNPs and OS; (D−F) MSCs were treated with OS only; (G−I) MSCs were treated with OS and 1.0 nM AuNPs. The images are representative of three independent experiments.

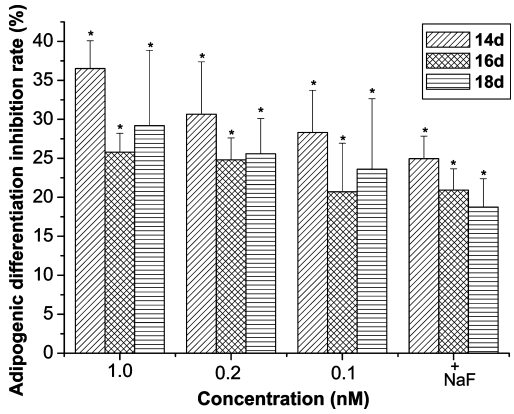

Figure 4. Dose-dependence of AuNPs on the adipogenic differentiation inhibition of MSCs. Results are mean ± SD of the triplicate experiments: (*) $p < 0.01$; 1.0 μM NaF was used as positive control.

tion of adipogenic differentiation. The effects of AuNPs on adipocytic differentiation of MSCs in the presence of adipogenic supplement (AS) were determined by specifically staining intracytoplasmic lipids with oil red O (Supporting Information, Figure S3A−3C). The results demonstrated a substantial inhibition effect on MSC adipocytic differentiation by AuNPs in time- and dose-dependent manners, where up to 35% inhibition was observed at the dosage of 1.0 nM AuNPs on day 14 and the inhibition rate decreased on day 16 and day 18 (Figure 4).

Osteogenic differentiation is a sequential event that follows initial cell proliferation. It is also possible that an increase in the rate of cell growth induced by AuNPs may result in the increasing level of MSC osteogenic differentiation. However, MTT assays revealed only a slight positive effect of AuNPs on MSC proliferation, where the cell viability was increased by 12 to 22% with no obvious dose- or time-dependent tendency (Figure 5A). Similarly, after 5 days of culture with the AuNPs, acridine orange staining of the live MSCs showed that cell number only slightly increased upon interactions with AuNPs (Figure 5B,C). The above results suggested that the cellular effects of AuNPs on MSCs were mainly through activating osteogenic differentiation and inhibiting adipogenic differentiation.

The interaction between MSCs and nanomaterials has been previously investigated.[27−30] It is commonly accepted that cells maintain their homeostasis through a comprehensive signaling network,[31] and any perturbation of this system by nanomaterials will influence cell function and behavior.[32,33] Incubation of nanomaterials with cells in culture media results in adsorption of serum proteins on the material surface, which induces the entry of nanomaterials into cells by receptor-mediated endocytosis.[34−36] Our TEM images confirmed that most of the AuNPs were grouped in intracellular compartments of cells (Figure 6E−H). Cells treated with OS in the absence of AuNPs displayed their typical ultrastructure characterized by a well-preserved plasma membrane, a nucleus with uniformly dispersed chromatin and clear nucleolus, and a cytoplasm containing randomly distributed organelles and electron-dense granules (Figure 6A−D). Cells exposed to AuNPs, on the other hand, seemed to incorporate the nanoparticles inside the cells in perinuclear compartments and vesicular structures close to the cell nucleus. The TEM images suggested that AuNPs may interact with proteins located in the cytoplasm, thus interfering with certain cellular signaling pathways.

Recent evidence showed that mechanical stimuli can regulate the direction of stem cell differentiation,[18−20] and several signaling molecules have been demonstrated to play significant roles in mechanical stimuli-initiated signal transduction.[37] Among them are the MAP kinases (MAPKs), which can be activated by mechanical stresses. Activation of MAPKs may link the effects of mechanical stress to the biochemical responses and gene expression.[18,38−40] There are also reports suggesting that MAPK pathways played critical roles in directing MSC commitment to the osteogenic

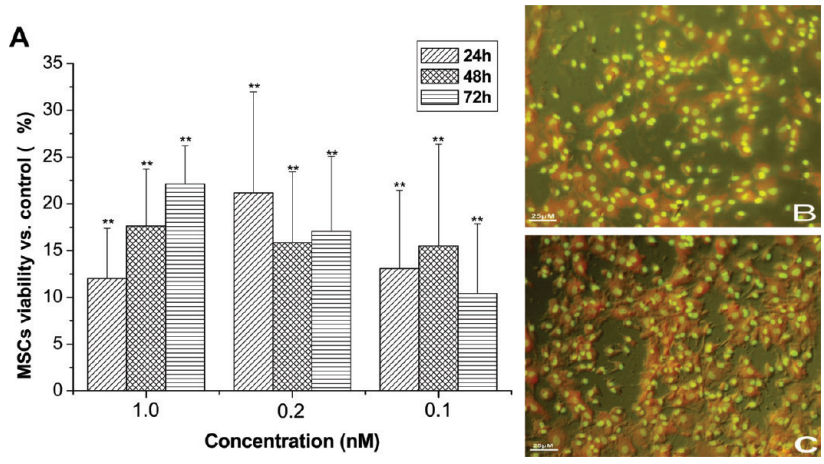

Figure 5. (A) Proliferation and viability of MSCs in the presence of 20 nm AuNPs. Results are mean ± SD of the triplicate experiments: (*) $p < 0.01$. The images of acridine orange staining show the MSCs without (B) and with (C) AuNPs treatment. The images are representative of three independent experiments.

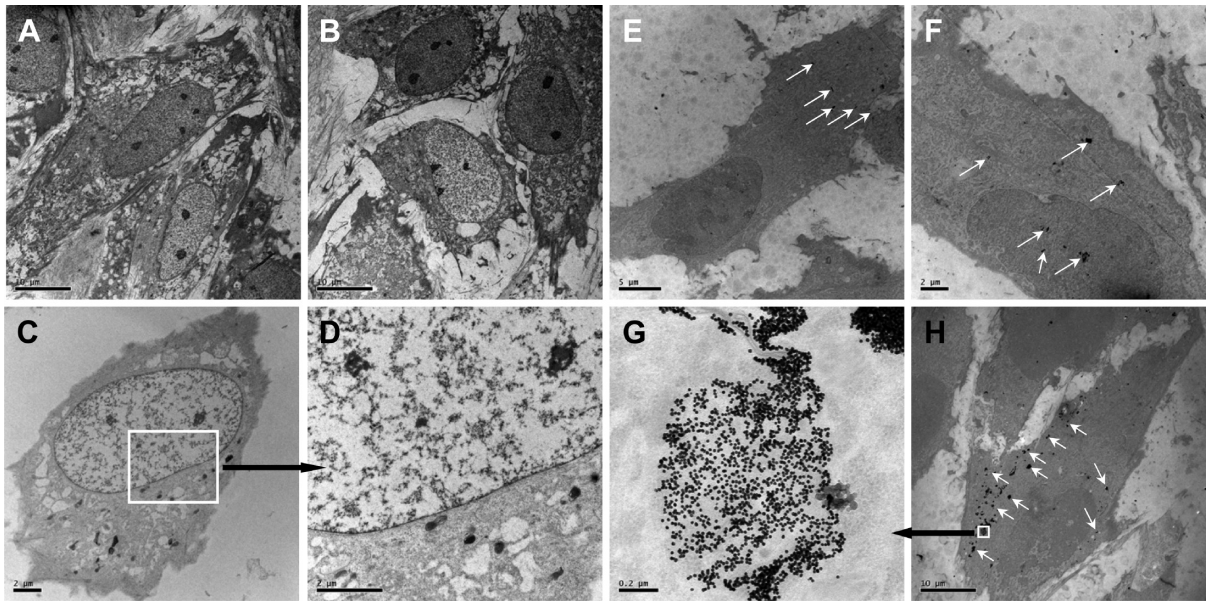

Figure 6. TEM images of the internalization of AuNPs. (A−D): Cells were treated with OS as control; (E−H): cells were treated with OS and 1.0 nM AuNPs. Arrows indicate AuNPs. The images are representative of three independent experiments.

lineage.[41−43] Therefore, we hypothesized that AuNPs may serve as mechanical stimuli on MSCs to activate MAPK signaling pathway in the cells and thus induce their preferential differentiation. Western blotting assays and RT-PCR experiments were thus carried out to verify the involvement of the MAPK pathways during AuNP−MSC interaction.

Three parallel pathways of MAPK have been described, including extracellular signal related kinases (ERK1/2), protein kinase 38 (p38), and c-Jun-N-terminal kinases (JNKs) pathways. JNK and p38 are often referred to as stress-activated protein kinases (SAPK1/JNK and SAPK2/p38), and ERK1/2 are often described as the kinases involved in growth factor stimulation.[44] The expression levels of key proteins involved in MAPK signaling pathway, including ERK1/2, p38, and JNK, were measured, and the results revealed that p38 protein was significantly up-regulated (Figure 7A). No substantial enhancement was observed for the expression of ERK1/2 and JNK proteins, suggesting that only p38 MAPK signaling pathway was activated in MSCs upon interaction with AuNPs (Figure 7A). Previous reports also demonstrated that p38 MAPK can positively regulate osteogenic differentiation.[45,46] It is known that phosphorylated p38 proteins can translocate into nucleus, bind to promoters of target genes, and regulate their transcription. The Western blotting results showed that MSCs exhibited an increase in the p38 phosphorylation level upon the treatment of AuNPs (Figure 7B).

Interconversion of MSCs among phenotypes, as well as the commitment to a particular lineage with suppression of alternative phenotypes, is governed by specific transcription factors. It has been established

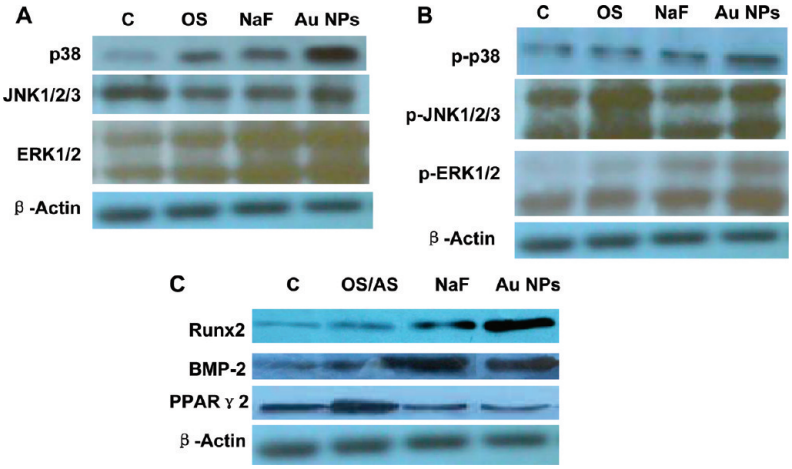

Figure 7. (A) Activation of p38 MAPK signaling induced by 1.0 nM AuNPs. (B) Phosphorylation of p38 MAPK after exposure to 1.0 nM AuNPs. (C) Western blot analysis for Runx2, BMP2, and PPARγ2 protein expression after exposure to 1.0 nM AuNPs. The blot shown is representative of three independent experiments.

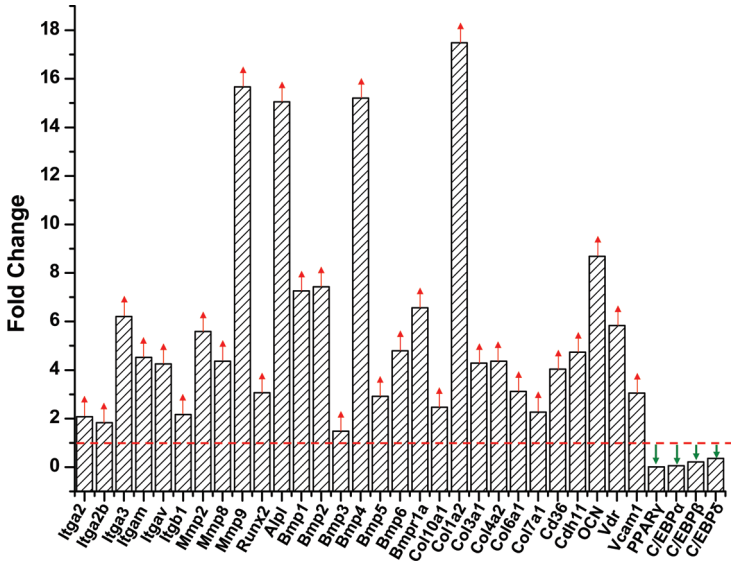

Figure 8. Real time RT-PCR analysis of osteogenic and adipogenic specific gene expression in MSCs upon treatment with 1.0 nM AuNPs.

that Runx2 determines the osteoblast lineage from the pluripotent MSCs,[47] while PPARγ destines cells to adipocyte differentiation.[48] BMP2 is a member of the TGF-β super family and plays a key regulatory role as a cell−cell signaling molecule during bone formation and repair.[49] Recent evidence has also shown that BMP2 played a crucial role in the regulation of osteogenic differentiation of MSCs on nanotopographic substrates.[13] As shown in Figure 7C, significant increase in Runx2 and BMP2 expression and substantial attenuation of PPARγ expression were observed, which is consistent with the observations in cellular assays that AuNPs preferentially promoted MSCs to differentiate into the osteoblastic phenotype rather than the adipocytic phenotype. A previous report has demonstrated that mechanical stress down-regulated PPARγ in MSCs and favored osteogenesis at the expense of adipogenesis.[50] The above results indicated that AuNPs might serve as mechanical stimuli to activate the p38 MAPK signaling pathway, thus triggering the expression of osteogenic genes underlying the phenotype of terminally differentiated osteocytes.

Real-time RT-PCR experiments were carried out to measure the transcriptional profile of osteospecific genes, and the up-regulation of 74 osteogenic marker genes was observed in MSCs treated with AuNPs (Figure 8, also see Supporting Information, Figure S4 and Table S1 for descriptions of all genes and their functions). Integrins, which are receptors of extracellular matrix, have been demonstrated to play a critical role in mechanical stress-induced p38 MAPK activation.[51] RT-PCR results showed substantial increase in the expression of integrin family genes (2.07, 1.83, 6.20, 4.52, and 4.25 fold increase for integrin α2, integrin α2b, integrin α3, integrin αM, and integrin αV, respectively), suggesting that integrins might also play a significant role in transmitting nanoparticle-induced mechanical stress across the plasma membrane. Matrix metalloproteases (Mmps) represent a family of endoproteinases which are able to cleave virtually all components of the extracellular matrix and other substrates such as growth factor binding proteins or latent growth factors, thus regulating their bioavailability.[52] A recent study showed that Mmps played an essential role in transferring environmental mechanical stimuli into MSCs.[53] Therefore, the significant increase in the expression of Mmp genes (5.59, 4.37, and 15.67-fold increase for Mmp2, Mmp8, and Mmp9, respectively) provided other evidence that AuNPs exert their effect through mechanical stress. The lineage commitment gene Runx2, which determines the osteoblast lineage from the pluripotent MSCs, showed a 3.06-fold increase when MSCs were treated with AuNPs. This is consistent with the Western blotting result (Figure 7C) and previous studies that mechanical stress could directly up-regulate the expression of Runx2.[40,43] The up-regulation of Runx2 is believed to be modulated by distinct MAPK cascades,[41] which subsequently up-regulates osteoblasts marker genes.[47] The osteogenic specific gene, ALPL, which plays vital roles in bone formation and mineralization, was up-regulated by 15.05 folds. As mentioned above, BMPs are responsible for enhancing osteoblastic differentiation, including stimulation of the expression of bone structural proteins such as Col-I and OCN, and the mineralization of bone matrix.[33,49] During the proliferation period, the genes associated with the formation of ECM components (such as type-I collagen and fibronectin) are activated. Type-I collagen is the most abundant protein found in the organic bone matrix and plays an essential role in influencing cellular behavior.[33] When the MSCs were exposed to AuNPs, the expression of BMP1, BMP2, BMP4, and Col1a2 were up-regulated by 7.26, 7.43, 15.21, and 17.48 folds, respectively. These results provided the molecular basis for our SEM observations that AuNPs induced MSCs to produce extracellular matrix and form modular structures (Figure 3). OCN which is expressed during the postproliferative period and reaches its maximum expression during mineralization and accumulates in the mineralized bone, showed a 8.60-fold increase when MSCs were treated with AuNPs.[24,33] Furthermore, the expression of cell−cell adhesion related genes (Cd36, Cdh11, and Vcam1) showed 4.04, 4.74, and 3.05-fold up-regulation, respectively. Overall, the transcriptional profile of osteogenic specific genes clearly illustrated the genetic events during the promotion of MSC osteogenic differentiation by AuNPs as observed in enhanced ALP activity (Figure 2A) and mineralized matrix nodules formation (Figure 2B).

The cellular assay results indicated that AuNPs also inhibited the adipogenesis of MSCs (Figure 4). Adipogenesis begins with the transient expression of CCAAT/

enhancer binding protein β (C/EBPβ) and C/EBPδ, which activate C/EBPα and PPARγ. C/EBPα and PPARγ together coordinate the expression of adipogenic genes underlying the phenotype of terminally differentiated adipocytes.[48] The expression of adipogenic specific genes and proteins is expected to be attenuated in MSCs upon AuNP treatment. RT-PCR and Western blot results clearly showed that MSCs cultured with AuNPs had significantly lower expression of these adipogenesis lineage commitment genes at both RNA (Figure 8) and protein level (Figure 7C). Previous reports also showed that mechanical stress can inhibit adipogenesis, which is associated with the down-regulation of related marker genes with a distinct expression profile.[54,55] The observed adipogenic transcriptional profile is thus consistent with our hypothesis, that AuNPs exert their effects on MSCs through mechanical stress.

On the basis of the above findings, a schematic model was proposed to describe the modulation of osteogenic differentiation of MSCs by AuNPs (Figure 9). AuNPs interact with the membrane of MSCs and bind with proteins in the cytoplasm after internalization through endocytosis, causing mechanical stress on the cells. The activation of p38 MAPK signaling pathway leads to the up-regulation of the osteogenic master transcription factor, Runx2,[40−43] and the down-regulation of the adipocytic master transcription factor, PPARγ.[50] Runx2 subsequently up-regulates osteoblast marker genes, Col I and BMP2 at early stages and ALP and OCN at later stages of differentiation,[33] thus driving MSCs to differentiate toward osteoblast cells.

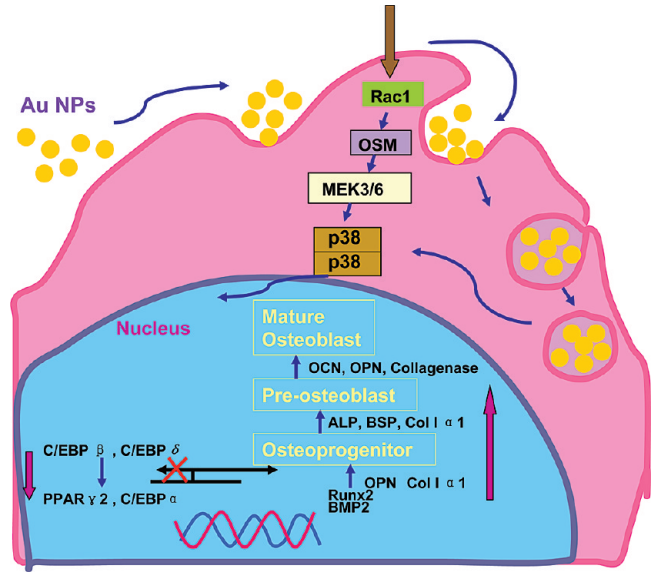

Figure 9. Molecular mechanism of the modulation of osteogenic and adipocytic differentiation of MSCs by AuNPs through p38 MAPK signaling pathway.

CONCLUSION

Our study showed that AuNPs promoted the osteogenic differentiation and inhibited the adipogenic differentiation of MSCs. TEM images suggested that AuNPs may interact with proteins located in the cytoplasm, thus interfering with certain cellular signaling pathways. The up-regulation of integrins indicated the interaction of AuNPs with the extracellular matrix. Both processes serve as mechanical stress on the MSCs, leading to the activation of the p38 MAPK signaling pathway, which in turn causes the up-regulation of osteogenic genes and the down-regulation of adipogenesis specific genes. The results described in this study revealed how AuNPs impact cellular events and the fate of stem cells, which will be important for the rational design of new nanomaterials for tissue engineering and other biomedical applications.

EXPERIMENTAL SECTION

Isolation and Culture of MSCs. MSCs were prepared from 6-week-old specific pathogen free (SPF) Kunming mice (Southern Medical University, China) following the Kelly method.[56,57] In brief, 6-week-old mice were executed by cervical vertebra. Femora and tibiae were aseptically harvested, and the whole bone marrow was flushed using supplemented DMEM in a 10-cc syringe and a 25-gauge needle. MSCs were collected and cultured in DMEM with 10% heat-inactivated fetal bovine serum, 100 U mL^{-1} penicillin (BBI, Canada), and 100 μg mL^{-1} streptomycin (BBI, Canada), for 3 days in a humidified atmosphere of 5% CO_2 in air at 37 °C (Sanyo, model MCO-18AIC), then replaced with fresh medium. The culture medium was changed every 3 days during the experiments.

Cellular Assays for MSC Proliferation and Differentiation. MSCs proliferation was determined using MTT assay, as described in detail previously.[58] Briefly, MSCs were seeded in 96-well tissue culture plates at the density of 4×10^6 cells per well and incubated for 3 days. After the addition of AuNPs at different concentrations (final concentration 0.1, 0.2, and 1.0 nM), 24, 48, and 72 h further incubations were performed. Then, the adherent cells were harvested for MTT assay. Briefly, 20 μL of MTT (5.0 mg mL^{-1} in 1× phosphate buffered saline (PBS)) was added and incubated for another 4 h at 37 °C. The supernatant was removed, and DMSO was added to each well for 10 min to dissolve any resulting formazan crystals. The absorbance was read at 550 nm using a microplate spectrophotometer (Biorad model 680, USA). Cells without AuNPs treatment were used as control. The relative cytotoxicity was expressed as a percentage: $[OD_{sample} - OD_{control}]/[OD_{control}] \times 100$.

ALP activity assay and ARS staining assay were employed to evaluate the osteogenic differentiation of MSCs.[33] For ALP assay, MSCs were seeded in 48-well tissue culture plates at the density of 5×10^6 cells per well with the osteogenetic induction supplement (OS) containing 5.0 mM β-glycerophosphate (BBI, Canada) and 50 μg mL^{-1} ascorbic acid (Sigma, USA) and 0.1 μM dexamethasone (Sigma, USA). A series of dilutions of AuNPs (final concentration 0.1, 0.2, and 1.0 nM) were added to the culture medium with OS in 48-well plates for 7, 10, and 14 days. NaF (Sigma, USA), which can promote osteogenetic differentiation of MSCs, was used as a positive control and dispersed in α-MEM.[59] After incubation, MSCs were washed twice with ice-cold D-Hank's and lysed by two cycles of freezing and thaw. Aliquots of supernatants were subjected to ALP activity and protein content measurement by an ALP activity kit (Nanjing Jiancheng Biological Engineering Institute, China) and a micro-Bradford assay kit (Beyotime Biotechnology, China).[57] For ARS staining assay, MSCs (5×10^6 cells per well) were seeded in 48-well tissue cul-

ture plates and cultured for 3 days. The medium was then changed to medium containing OS and AuNPs (final concentration 0.1, 0.2, and 1.0 nM) or 1.0 μM NaF for 9, 15, and 21 days. The formation of mineralized matrix nodules was determined by ARS staining.[60] In brief, MSCs were fixed in 70% ethanol for 1 h and then stained with 40 mM ARS (pH 4.2, Sigma, USA) for 30 min at room temperature. Quantification of alizarin red S staining was performed by elution with 10% (w/v) cetylpyridium chloride (Sigma, USA) for 10 min and measurement of the absorbance at 570 nm.[57] The mineralization inhibition rate was expressed as a percentage: $[OD_{sample} - OD_{control}]/[OD_{control}] \times 100$.

The adipocytic differentiation rates of MSCs in the absence and presence of AuNPs were determined by specifically staining intracytoplasmic lipids with oil red O.[61] MSCs (1×10^7 cells per well) were seeded in 48-well tissue culture plates and cultured for 14, 16, and 18 days. The adipogenetic induction supplements (10 mg L^{-1} insulin, 0.1 μM dexamethasone) and AuNPs (final concentration 0.1, 0.2, and 1.0 nM) were added to the culture medium. After incubation, MSCs were washed by D-Hank's twice and then stained by 0.6% (w/v) oil red O (Sigma, USA) solution (60% isopropyl alcohol, 40% water) for 15 min. For quantification of oil red O content, MSCs were washed with D-Hank's three times to remove background staining and isopropyl alcohol was added to resolve oil red O. Absorbance at 510 nm was measured on a microplate spectrophotometer (Biorad model 680, USA). The adipogenetic differentiation inhibition was expressed as a percentage: $[OD_{sample} - OD_{control}]/[OD_{control}] \times 100$.

SEM and TEM. Cell morphology with and without the treatment of 1.0 nM AuNPs was observed by SEM after 7 days of culture, as described in detail elsewhere.[33,62,63] In brief, MSCs were soaked in modified Karnovsky fixative (2% glutaraldehyde +2% paraformaldehyde) in 0.1 M cacodylate buffer (pH 7.4) with 0.05% $CaCl_2$ solution at 4 °C for 2 h and postfixed for 1 h at 4 °C with 1% osmium tetroxide before dehydration with increasing concentrations of ethanol, and finally with hexamethyldisilazane (HMDS) to further extract water. The dehydrated MSCs were maintained in desiccators for overnight air drying. After sputter-coating with carbon, SEM imaging was conducted on FEI Nova SEM system at accelerating voltage of 10 kV. The ultrastructural alterations and internalization of MSCs after 7 days of culture in the presence of 1.0 nM AuNPs were observed with a Phillips Tecnai 12 instrument operating at 80 kV, as described in detail elsewhere.[33] In brief, MSCs were prefixed in modified Karnovsky fixative (2% glutaraldehyde + 2% paraformaldehyde) in 0.1 M cacodylate buffer (pH 7.4) with 0.05% $CaCl_2$ solution at 4 °C for 2 h. The cells were then postfixed in 1% osmium tetroxide, subsequently dehydrated in a graded series of ethanol and acetone solution, and embedded in resin. Ultrathin sections were performed, collected on copper grids, and stained with 5% uranyl acetate in water for 4 min and lead citrate for 2 min. All SEM and TEM microscopic related reagents were obtained from Electron Microscopy Sciences, USA.

Molecular Assays for Mechanism Study. Western blots and RT-PCR were employed to study protein and gene expression of MSCs upon their interactions with 1.0 nM AuNPs, as described in detailed previously.[64] A Western blot can be used to detect a specific protein expression in a given sample. Proteins were subjected to SDS-PAGE using 10% gel for the detection of ERK1/2, p-ERK1/2, p38, p-p38, JNK, p-JNK, Runx2, BMP2, and PPARγ2, and transferred onto a nitrocellulose membrane (Amersham Biosciences, UK). The membrane was blocked overnight at 4 °C. Then, the blots were incubated with corresponding primary antibodies (GeneLinx International, Inc.) in the TBST solution for 2 h at room temperature, followed by 1 h incubation with secondary antibodies conjugated with horseradish peroxidase. Membranes were exposed for 15−30 min to Hyperfilm (Amersham Biosciences, UK) for detection of signals. β-Actin protein expression was used as a loading control.

Total RNA from MSCs which were treated with 1.0 nM AuNPs in the presence of OS for 7 days was extracted using Trizol Plus RNA purification kit (Invitrogen), and was reverse transcribed to first-strand cDNA according to the TaKaRa protocol (TaKaRa, Tokyo). An RT^2ProfilerPCR Array System containing 84 relevant, pathway-focused genes of osteogenesis was performed using ABI 7000 Sequence Detection System (Applied Biosystems, USA). A 25 μL portion of the experiment cocktail containing 13 μL of SABiosciences RT^2 qPCR Master Mix (SABiosciences, USA), 1 μL of cDNA and 11 μL of ddH_2O was added to each well where the gene-specific primer used for RT-PCR was immobilized. PCR products were analyzed with PCR array data analysis web portal from the following address: http://www.SABiosciences.com/pcrarraydataanalysis.php. RT-PCR was performed in a total volume of 25 μL with 1 μL of cDNA, 1 μL of gene-specific 10 μM PCR primer pair stock, and 12.5 μL of SYBR Green/ROX Master Mix (SABiosciences, USA) using ABI 7000 Sequence Detection System (Applied Biosystems, USA). The PCR profile began with 10 min at 95 °C to activate Hotstart TaqDNA polymerase, followed by 40 cycles of 15 s at 95 °C and 1 min at 60 °C, and later followed by the melting curve test. The relative amount of mRNA expression normalized to GAPDH was expressed as fold change, which was calculated by the comparative CT ($2^{-\Delta\Delta CT}$) relative to control group as a reference: $2^{-\Delta\Delta CT} = 1$. The primers used for RT-qPCR are OCN, 5′-GAACAGACTCCGGCGCTA-3′, 5′-AGGGAGGATCAAGTCCCG-3′; PPARγ2, 5′-TGTGGGGATAA AGCATCAGGC-3′, 5′-CCGGCAGTTAAGATCACACCTAT-3′; C/EBPα, 5′-GTGCTTCATGGAGCA AGCCAA-3′, 5′-TGTCGATGGAGTGCTCGTTCT-3′; C/EBPβ, 5′-GCGCGAGCGCAACAACATCG-3′, 5′-CAGCACAGGCTGTTGACCATCATA-3′; C/EBPδ, 5′-GAGCGTCCTACGCGCCAGTAC-3′, 5′-GATCACGGAGCTGTGCCGGTC-3′.

Statistical Analysis. Data were collected from three separate experiments and expressed as mean ± standard deviation (SD). The statistical differences were analyzed by a paired Student's *t*-test; *p* values less than 0.05 were considered to indicate statistical differences.

Acknowledgment. The financial support from Shenzhen Double 100 Science and Technology Project, National Natural Science Foundation of China (Project No. 20971034) and the Innovation and Technology Fund (Project No. ITS/353/09) is gratefully acknowledged.

Supporting Information Available: Additional figures and a table of the 74 osterogenic differentiation specific genes that are up-regulated in MSCs upon their interactions with 1.0 nM AuNPs.

This material is available free of charge *via* the Internet at http://pubs.acs.org.

REFERENCES AND NOTES

1. Pittenger, M. F.; Mackay, A. M.; Beck, S. C.; Jaiswal, R. K.; Douglas, R.; Mosca, J. D.; Moorman, M. A.; Simonetti, D. W.; Craig, S.; Marshak, D. R. Multilineage Potential of Adult Human Mesenchymal Stem Cells. *Science* **1999**, *284*, 143–147.
2. Jiang, Y.; Jahagirdar, B. N.; Reinhardt, R. L.; Schwartz, R. E.; Keene, C. D.; Ortiz-Gonzalez, X. R.; Reyes, M.; Lenvik, T.; Lund, T.; Blackstad, M.; *et al*. Pluripotency of Mesenchymal Stem Cells Derived from Adult Marrow. *Nature* **2002**, *413*, 41–49.
3. Oreffo, R. O. C.; Cooper, C.; Mason, C.; Clements, M. Mesenchymal Stem Cells: Lineage, Plasticity and Skeletal Therapeutic Potential. *Stem. Cell. Rev.* **2005**, *1*, 169–178.
4. Alhadlaq, A.; Mao, J. J. Mesenchymal Stem Cells: Isolation and Therapeutics. *Stem Cells Dev.* **2004**, *13*, 436–448.
5. Colter, D. C.; Sekiya, I.; Prockop, D. J. Identification of a Subpopulation of Rapidly Self-Renewing and Multipotential Adult Stem Cells in Colonies of Human Marrow Stromal Cells. *Proc. Natl. Acad. Sci. U.S.A.* **2001**, *98*, 7841–7845.
6. Bianco, P.; Robey, P. G. Stem Cells in Tissue Engineering. *Nature* **2001**, *414*, 118–121.
7. Li, W. J.; Tuli, R.; Huang, X. X.; Laquerriere, P.; Tuan, R. S. Multilineage Differentiation of Human Mesenchymal Stem Cells in a Three-Dimensional Nanofibrous Scaffold. *Biomaterials* **2005**, *26*, 5158–5166.
8. Xin, X. J.; Hussain, M.; Mao, J. J. Continuing Differentiation of Human Mesenchymal Stem Cells and Induced

Chondrogenic and Osteogenic Lineages in Electrospun PLGA Nanofiber Scaffold. *Biomaterials* **2007**, *28*, 316–325.
9. Marletta, G.; Ciapetti, G.; Satriano, C.; Perut, F.; Salerno, M.; Baldini, N. Improved Osteogenic Differentiation of Human Marrow Stromal Cells Cultured on Ion-Induced Chemically Structured Poly-ϵ-caprolactone. *Biomaterials* **2007**, *28*, 1132–1140.
10. Prabhakaran, M. P.; Venugopal, J. R.; Ramakrishna, S. Mesenchymal Stem Cell Differentiation to Neuronal Cells on Electrospun Nanofibrous Substrates for Nerve Tissue Engineering. *Biomaterials* **2009**, *30*, 4996–5003.
11. Xin, Y. C.; Jiang, J.; Huo, K. F.; Hu, T.; Chu, P. K. Bioactive $SrTiO_3$ Nanotube Arrays: Strontium Delivery Platform on Ti-Based Osteoporotic Bone Implants. *ACS Nano* **2009**, *3*, 3228–3234.
12. Kaur, G.; Valarmathi, M. T.; Potts, J. D.; Wang, Q. The Promotion of Osteoblastic Differentiation of Rat Bone Marrow Stromal Cells by a Polyvalent Plant Mosaic Virus. *Biomaterials* **2008**, *29*, 4074–4081.
13. Kaur, G.; Valarmathi, M. T.; Potts, J. D.; Jabbari, E.; Sabo-Attwood, T.; Wang, Q. Regulation of Osteogenic Differentiation of Rat Bone Marrow Stromal Cells on 2D Nanorod Substrates. *Biomaterials* **2010**, *31*, 1732–1741.
14. Kaur, G.; Wang, C.; Sun, J.; Wang, Q. The Synergistic Effects of Multivalent Ligand Display and Nanotopography on Osteogenic Differentiation of Rat Bone Marrow Stem Cells. *Biomaterials* **2010**, *31*, 5813–5824.
15. Oliveira, J. M.; Sousa, R. A.; Kotobuki, N.; Tadokoro, M.; Hirose, M.; Mano, J. F.; Reis, R. L.; Ohgushi, H. The Osteogenic Differentiation of Rat Bone Marrow Stromal Cells Cultured with Dexamethasone-Loaded Carboxymethylchitosan/Poly(Amidoamine) Dendrimer Nanoparticles. *Biomaterials* **2009**, *30*, 804–813.
16. Green, D. E.; Longtin, J. P.; Sitharaman, B. The Effect of Nanoparticle-Enhanced Photoacoustic Stimulation on Multipotent Marrow Stromal Cells. *ACS Nano* **2009**, *3*, 2065–2072.
17. Gonzalez-McQuire, R.; Green, D. W.; Partridge, K. A.; Oreffo, R. O. C.; Mann, S.; Davis, S. A. Coating of Human Mesenchymal Cells in 3D Culture with Bioinorganic Nanoparticles Promotes Osteoblastic Differentiation and Gene Transfection. *Adv. Mater.* **2007**, *19*, 2236–2240.
18. Kumar, A.; Chaudhry, I.; Reid, M. B.; Boriek, A. M. Distinct Signaling Pathways Are Activated in Response to Mechanical Stress Applied Axially and Transversely to Skeletal Muscle Fibers. *J. Biol. Chem.* **2002**, *277*, 46493–46503.
19. Datta, N.; Pham, Q. P.; Sharma, U.; Sikavitsas, V. I.; Jansen, J. A.; Mikos, A. G. *In vitro* Generated Extracellular Matrix and Fluid Shear Stress Synergistically Enhance 3d Osteoblastic Differentiation. *Proc. Natl. Acad. Sci. U.S.A.* **2006**, *103*, 2488–2493.
20. Discher, D. E.; Mooney, D. J.; Zandstra, P. W. Growth Factors, Matrices, and Forces Combine and Control Stem Cells. *Science* **2009**, *324*, 1673–1677.
21. Yao, H.; Yi, C. Q.; Tzang, C. H.; Zhu, J. J.; Yang, M. S. DNA-Directed Self-Assembly of Gold Nanoparticles into Binary and Ternary Nanostructures. *Nanotechnology* **2007**, *18*, 015102.
22. Chow, M. K.; Zukoski, C. F. Gold Sol Formation Mechanisms: Role of Colloidal Stability. *J. Colloid Interface Sci.* **1994**, *165*, 97–109.
23. Pockwinse, S.; Wilming, L.; Conlon, D.; Stein, G. S.; Lian, J. B. Expression of Cell-Growth and Bone Specific Genes at Single Cell Resolution during Development of Bone Tissue-Like Organization in Primary Osteoblast Cultures. *J. Cell. Biochem.* **1992**, *49*, 310–323.
24. Abdallah, B. M.; Jensen, C. H.; Gutierrez, G.; Leslie, R. G. Q.; Jensen, T. G.; Kassem, M. Regulation of Human Skeletal Stem Cells Differentiation by Dlk1/Pref-1. *J. Bone. Miner. Res.* **2004**, *19*, 841–852.
25. Stein, G. S.; Lian, J. B. Molecular Mechanisms Mediating Proliferation/Differentiation Interrelationships during Progressive Development of the Osteoblast Phenotype. *Endocr. Rev.* **1993**, *14*, 424–442.
26. Popat, K. C.; Chatvanichkul, K. I.; Barnes, G. L.; Latempa, T. J.; Grimes, C. A.; Desai, T. A. Osteogenic Differentiation of Marrow Stromal Cells Cultured on Nanoporous Alumina Surfaces. *J. Biomed. Mater. Res. Part A* **2006**, *80A*, 955–964.
27. Mooney, E.; Dockery, P.; Greiser, U.; Murphy, M.; Barron, V. Carbon Nanotubes and Mesenchymal Stem Cells: Biocompatibility, Proliferation and Differentiation. *Nano Lett.* **2008**, *8*, 2137–2143.
28. Rajan, S. S.; Liu, H. Y.; Vu, T. Q. Ligand-Bound Quantum Dot Probes for Studying the Molecular Scale Dynamics of Receptor Endocytic Trafficking in Live Cells. *ACS Nano* **2008**, *2*, 1153–1166.
29. Seleverstov, O.; Zabirnyk, O.; Zscharnack, M.; Bulavina, L.; Nowicki, M.; Heinrich, J. M.; Yezhelyev, M.; Emmrich, F.; O'Regan, R.; Bader, A. Quantum Dots for Human Mesenchymal Stem Cells Labeling. A Size-Dependent Autophagy Activation. *Nano Lett.* **2006**, *6*, 2826–2832.
30. Lee, K. Y.; Alsberg, E.; Hsiong, S.; Comisar, W.; Linderman, J.; Ziff, R.; Mooney, D. Nanoscale Adhesion Ligand Organization Regulates Osteoblast Proliferation and Differentiation. *Nano Lett.* **2004**, *4*, 1501–1506.
31. White, M. A.; Anderson, R. G. W. Signaling Networks in Living Cells. *Annu. Rev. Pharmacol. Toxicol.* **2005**, *45*, 587–603.
32. Mu, Q. X.; Du, G. Q.; Chen, T. S.; Zhang, B.; Yan, B. Suppression of Human Bone Morphogenetic Protein Signaling by Carboxylated Single-Walled Carbon Nanotubes. *ACS Nano* **2009**, *3*, 1139–1144.
33. Liu, D. D.; Yi, C. Q.; Zhang, D. W.; Zhang, J. C.; Yang, M. S. Inhibition of Proliferation and Differentiation of Mesenchymal Stern Cells by Carboxylated Carbon Nanotubes. *ACS Nano* **2010**, *4*, 2185–2195.
34. Yi, C. Q.; Fong, C. C.; Chen, W. W.; Qi, S. J.; Tzang, C. H.; Lee, S. T.; Yang, M. S. Interactions between Carbon Nanotubes and DNA Polymerase and Restriction Endonucleases. *Nanotechnology* **2007**, *18*, 025102.
35. Mu, Q. X.; Broughton, D. L.; Yan, B. Endosomal Leakage and Nuclear Translocation of Multiwalled Carbon Nanotubes: Developing a Model for Cell Uptake. *Nano Lett.* **2009**, *9*, 4370–4375.
36. Porter, A. E.; Gass, M.; Bendall, J. S.; Muller, K.; Goode, A.; Skepper, J. N.; Midgley, P. A.; Welland, M. Uptake of Noncytotoxic Acid-Treated Single-Walled Carbon Nanotubes into the Cytoplasm of Human Macrophage Cells. *ACS Nano* **2009**, *3*, 1485–1492.
37. Rubin, J.; Rubin, C.; Jacobs, C. R. Molecular Pathways Mediating Mechanical Signaling in Bone. *Gene* **2006**, *367*, 1–16.
38. Suzuma, I.; Suzuma, K.; Ueki, K.; Hata, Y.; Feener, E. P.; King, G. L.; Aiello, L. P. Stretch-Induced Retinal Vascular Endothelial Growth Factor Expression Is Mediated by Phosphatidylinositol 3-Kinase and Protein Kinase C (PKC)-ζ but Not by Stretch-Induced ERK1/2, Akt, Ras, or Classical/Novel PKC Pathways. *J. Biol. Chem.* **2002**, *277*, 1047–1057.
39. Keila, S.; Pitaru, S.; Grosskopf, A.; Weinreb, M. Bone-Marrow from Mechanically Unloaded Rat Bones Expresses Reduced Osteogenic Capacity *in Vitro*. *J. Bone Miner. Res.* **1994**, *9*, 321–327.
40. Wang, F. S.; Wang, C. J.; Sheen-Chen, S. M.; Kuo, Y. R.; Chen, R. F.; Yang, K. D. Superoxide Mediates Shock Wave Induction of ERK-Dependent Osteogenic Transcription Factor (CBFA1) and Mesenchymal Cell Differentiation toward Osteoprogenitors. *J. Biol. Chem.* **2002**, *277*, 10931–10937.
41. Xiao, G.; Jiang, D.; Thomas, P.; Benson, M. D.; Guan, K.; Karsenty, G.; Franceschi, R. T. MAPK Pathways Activate and Phosphorylate the Osteoblast-Specific Transcription Factor, Cbfa1. *J. Biol. Chem.* **2000**, *275*, 4453–4459.
42. Jaiswal, R. K.; Jaiswal, N.; Bruder, S. P.; Mbalaviele, G.; Marshak, D. R.; Pittenger, M. F. Adult Human Mesenchymal Stem Cell Differentiation to the Osteogenic or Adipogenic Lineage Is Regulated by Mitogen-Activated Protein Kinase. *J. Biol. Chem.* **2000**, *275*, 9645–9652.
43. Ziros, P. G.; Gil, A. P.; Georgakopoulos, T.; Habeos, I.;

Kletsas, D.; Basdra, E. K.; Papavassiliou, A. G. The Bone-Specific Transcriptional Regulator Cbfa1 Is a Target of Mechanical Signals in Osteoblastic Cells. *J. Biol. Chem.* **2002**, *277*, 23934–23941.
44. Chang, L. F.; Karin, M. Mammalian MAP Kinase Signalling Cascades. *Nature* **2001**, *410*, 37–40.
45. Li, X. T.; Udagawa, N.; Itoh, K.; Suda, K.; Murase, Y.; Nishihara, T.; Suda, T.; Takahashi, N. p38 MAPK-Mediated Signals Are Required for Inducing Osteoclast Differentiation but Not for Osteoclast Function. *Endocrinology* **2002**, *143*, 3105–3113.
46. Guicheux, J.; Lemonnier, J.; Ghayor, C.; Suzuki, A.; Palmer, G.; Caverzasio, J. Activation of p38 Mitogen-Activated Protein Kinase and c-Jun-NH_2-Terminal Kinase by BMP-2 and Their Implication in the Stimulation of Osteoblastic Cell Differentiation. *J. Bone. Miner. Res.* **2003**, *18*, 2060–2068.
47. Komori, T. Requisite roles of Runx2 and Cbfb in Skeletal Development. *J. Bone. Miner. Metab.* **2003**, *21*, 193–197.
48. Zhang, W. X.; Yang, N. L.; Shi, X. M. Regulation of Mesenchymal Stem Cell Osteogenic Differentiation by Glucocorticoid-Induced Leucine Zipper (GILZ). *J. Biol. Chem.* **2008**, *283*, 4723–4729.
49. Benoit, D. S. W.; Collins, S. D.; Anseth, K. S. Multifunctional Hydrogels That Promote Osteogenic Human Mesenchymal Stem Cell Differentiation through Stimulation and Sequestering of Bone Morphogenic Protein 2. *Adv. Funct. Mater.* **2007**, *17*, 2085–2093.
50. David, V.; Martin, A.; Lafage-Proust, M. H.; Malaval, L.; Peyroche, S.; Jones, D. B.; Vico, L.; Guignandon, A. Mechanical Loading down-Regulates Peroxisome Proliferator-Activated Receptor Gamma in Bone Marrow Stromal Cells and Favors Osteoblastogenesis at the Expense of Adipogenesis. *Endocrinology* **2007**, *148*, 2553–2562.
51. Aikawa, R.; Nagai, T.; Kudoh, S.; Zou, Y. Z.; Tanaka, M.; Tamura, M.; Akazawa, H.; Takano, H.; Nagai, R.; Komuro, I. Integrins Play a Critical Role in Mechanical Stress-Induced p38 MAPK Activation. *Hypertension* **2002**, *39*, 233–238.
52. Sternlicht, M. D.; Werb, Z. How Matrix Metalloproteinases Regulate Cell Behavior. *Annu. Rev. Cell. Dev. Biol.* **2001**, *17*, 463–516.
53. Kasper, G.; Glaeser, J. D.; Geissler, S.; Ode, A.; Tuischer, J.; Matziolis, G.; Perka, C.; Duda, G. N. Matrix Metalloprotease Activity Is an Essential Link between Mechanical Stimulus and Mesenchymal Stem Cell Behavior. *Stem Cells* **2007**, *25*, 1985–1994.
54. Rubin, C. T.; Capilla, E.; Luu, Y. K.; Busa, B.; Crawford, H.; Nolan, D. J.; Mittal, V.; Rosen, C. J.; Pessin, J. E.; Judex, S. Adipogenesis Is Inhibited by Brief, Daily Exposure to High-Frequency, Extremely Low-Magnitude Mechanical Signals. *Proc. Natl. Acad. Sci. U.S.A.* **2007**, *104*, 17879–17884.
55. Sen, B.; Styner, M.; Xie, Z. H.; Case, N.; Rubin, C. T.; Rubin, J. Mechanical Loading Regulates NFATc1 and β-Catenin Signaling through a GSK3 Beta Control Node. *J. Bio. Chem.* **2009**, *284*, 34607–34617.
56. Kelly, K. A.; Gimble, J. M. 1,25-Dihydroxy Vitamin D_3 Inhibits Adipocyte Differentiation and Gene Expression in Murine Bone Marrow Stromal Cell Clones and Primary Cultures. *Endocrinology.* **1998**, *139*, 2622–2628.
57. Zhang, D. W.; Yi, C. Q.; Zhang, J. C.; Chen, Y.; Yao, X. S.; Yang, M. S. The Effects of Carbon Nanotubes on the Proliferation and Differentiation of Primary Osteoblasts. *Nanotechnology* **2007**, *18*, 475102.
58. Carmichael, J.; Degraff, W. G.; Gazdar, A. F.; Minna, J. D.; Mitchell, J. B. Evaluation of a Tetrazolium-Based Semiautomated Colorimetric Assay—Assessment of Chemosensitivity Testing. *Cancer. Res.* **1987**, *47*, 936–942.
59. Farley, J. R.; Barlink, D. J.; Barlink, D. J. Fluoride Directly Stimulates Proliferation and Alkaline Phosphatase Activity of Bone-Forming Cells. *Science* **1983**, *4621*, 330–332.
60. Gori, F.; Divieti, P.; Demay, M. Cloning and Characterization of a Novel WD-40 Repeat Protein That Dramatically Accelerates Osteoblastic Differentiation. *J. Biol. Chem.* **2001**, *276*, 46515–46522.
61. Sekiya, I.; Larson, B. L.; Smith, J. R.; Pochampally, R.; Cui, J. G.; Prockop, D. J. Expansion of Human Adult Stem Cells from Bone Marrow Stroma: Conditions That Maximize the Yields of Early Progenitors and Evaluate Their Quality. *Stem. Cells.* **2002**, *20*, 530–541.
62. Qi, S. J.; Yi, C. Q.; Chen, W. W.; Fong, C. C.; Lee, S. T.; Yang, M. S. Effects of Silicon Nanowires on HepG2 Cell Adhesion and Spreading. *ChemBioChem.* **2007**, *8*, 1115–1118.
63. Qi, S. J.; Yi, C. Q.; Fong, C. C.; Ji, S. L.; Yang, M. S. Cell Adhesion and Spreading Behavior on Vertically Aligned Silicon Nanowire Arrays. *ACS Appl. Mater. Interfaces* **2009**, *1*, 30–34.
64. Dalby, M. J.; Gadegaard, N.; Tare, R.; Andar, A.; Riehle, M. O.; Herzyk, P.; Wilkinson, C. D. W.; Oreffo, R. O. C. The Control of Human Mesenchymal Cell Differentiation Using Nanoscale Symmetry and Disorder. *Nat. Mater.* **2007**, *6*, 997–1003.